PHYSICAL REVIEW B VOLUME 18, NUMBER 8 15 OCTOBER 1978

Multipole wave functions for photoelectrons in crystals. II. Examples of constant-energy-surface harmonics. Application to the s-d bands of Cu

G. Strinati
Department of Physics, University of Chicago, Chicago, Illinois 60637
(Received 24 October 1977)

We construct a complete set of multipole wave functions for an electron in a crystral, appropriate to describe single-center phenomena. The set consists of superpositions of the Bloch waves of given energy E, weighted by a set of harmonics which is complete and orthonormal over the constant-energy surface $E_\mu(\vec{k}) = E$. We give prescriptions to label these harmonics. Numerical examples are discussed for the s-d bands of Cu. The case of a spherical constant-energy surface, whose harmonics are the spherical harmonics, reappears as a degenerate limit.

I. INTRODUCTION

A few years ago Fano suggested[1,2] a generalization of concepts and techniques of the quantum-defect theory of atomic and molecular spectra to describe single-center phenomena occurring in crystalline solids, namely, photoabsorption from inner shells and isolated impurities. The initial implementation of that approach[3] did not include applications and was subject to restrictions that are lifted in the present and in its companion paper. One can find in the recent literature both theoretical[4] and experimental[5] instances in favor of a relatively simple theory which would connect atomiclike effects and band properties. While we are still far from a direct comparison with the experimental evidence, we feel encouraged to report on the substantial progress that has been made thus far. This introductory section describes our theoretical approach.

As the presence of a localized "center" spoils the translational symmetry of the Hamiltonian operator, the final state of a photoelectron cannot be simply described by a single Bloch wave, an eigenfunction of the perfect crystal Hamiltonian. The effect of the vacancy created by photoionization is assumed to be *localized* within a few crystal cells about the "central" cell. We then divide the crystal into two regions: (i) an *internal region* which is perturbed; (ii) an *external region* where the crystal is unperturbed. The two regions can be treated with different approaches[6]: (a) in the internal region we shall have to perform the numerical integration of a molecular-type many-body Schrödinger equation; (b) in the external region the solution can be expressed *analytically* in terms of the eigenfunctions of the unperturbed problem, i.e., Bloch waves. Owing to the exclusion of a finite volume, $\vec{k}$ vectors belonging to the Brillouin zone Ω must now be complemented by complex $\vec{k}$ vectors. Using a standard technique of mathematical physics, we will expand a general solution in the external zone, about its center, into an appropriate, complete set of multipole waves and then identify that particular solution which joins smoothly to the internal zone solution. To this end, we have to develop concepts and techniques which will enable us to match a molecularlike problem (internal region) to the description of a uniform crystalline medium (external region).

Earlier studies of scattering by a potential of finite range in a crystal[7] have presented contrasting features. Basically one follows the Lippmann-Schwinger formalism in which the wave function of the scattered particle is identified at *large* distances from a localized potential with reference to a particular $\vec{k}$ vector. On the other hand, the Bloch waves are then expanded into Wannier functions which are deemed appropriate to the treatment of a localized perturbation. These studies, however, do not discuss the effect of the long tails of the Wannier functions which are related to singular behavior of the Bloch waves in the proximity of loci of degeneracy in $\vec{k}$ space. These two aspects will be reconciled in our approach by considering superpositions of Lippmann-Schwinger solutions identified by different $\vec{k}$ vectors which *smooth out* the effect of singularities and thus confine the importance of the tails of the Wannier functions. It follows indeed from the complementarity of position and wave vector that singularities of Bloch functions in a limited region of $\vec{k}$ space are not very relevant to the effects of a perturbation localized in physical space.

The aim of the present paper is to show how the coefficients of the superpositions of Bloch waves [Eq. (2.3)] can be calculated in the case of a specific physical system, namely, copper. The quadratic interpolation scheme of Mueller *et al.*[8] has been adopted for this purpose because of its built-in smoothing of the $\vec{k}$-space singularities. The study of the singularities itself involves broad questions of band theory (convergence of the Wannier series, symmetry classification of the Wan-

nier functions, phase normalization of the Bloch waves) which greatly exceed the scope of the present paper and are deferred to the following one.

The paper is organized as follows. Section II introduces multipole wave functions and harmonics of the constant-energy surface in a crystal as the appropriate generalizations of the spherical Bessel functions and the spherical harmonics, respectively. Section III develops a recursion procedure which defines these harmonics and discusses the numerical techniques. In Sec. IV some characteristic features of the harmonics are analyzed for the case of copper.

II. MULTIPOLE WAVES: REGULAR SOLUTIONS

In the presence of an isolated impurity the Hamiltonian of the system loses the translational invariance characteristic of a perfect crystal but still possesses point-group symmetry about a central cell. (We consider for simplicity lattices with a single atom in each unit cell and a center of inversion at the atom.) As in a molecular problem, we classify the eigenfunctions of the Hamiltonian according to their energy and to the symmetry species to which they belong. We use the symbols Γ and i to indicate an irreducible representation of the point group of the lattice and one of its rows, respectively. Because the number of representations of finite groups and their dimensionalities are finite, we need additional indices, which range over an infinite set of values, in order to classify a complete set of *given energy* E.

In the course of this paper we restrict our attention to the subset of real $\vec{k}$ vectors belonging to the Brillouin zone Ω. Multipole waves with energy E, which are regular, i.e., not singular at the center, are then obtained by a unitary transformation of the solutions of the unperturbed crystal, i.e., of the set of Bloch waves $\{\varphi_\mu(\vec{r};\vec{k})\}$ with energy

$$E_\mu(\vec{k}) = E. \tag{2.1}$$

This relation defines a constant-energy surface in the Brillouin zone. We consider here one "band" at a time and allocate the eigensolutions to a particular band by using the ordered labeling.[9]

In order to separate energy and surface variables, the label $\vec{k}$ is replaced by the corresponding energy E and by orthogonal coordinates (ξ,η) over the constant-energy surface.[10] The Bloch waves are then normalized per unit range of the new continuous variables:

$$\varphi_\mu(\vec{r};E,\xi,\eta) = \left|\frac{\partial(k_x,k_y,k_z)}{\partial(E,\xi,\eta)}\right|^{1/2} \varphi_\mu(\vec{r};\vec{k}). \tag{2.2}$$

The unitary transformation connecting the set of Bloch waves $\{\varphi_\mu(\vec{r};E,\xi,\eta)\}$ to the corresponding set of multipole waves of given symmetry species, replaces the two continuous parameters (ξ,η) by an infinite set of indices, (L,q), whose meaning has been considered in Ref. 3. Indicating the unitary transformation by $\langle\xi\eta|\Gamma i L q\rangle_{E_\mu}$, we define the set of regular multipole waves by the prescription:

$$\mathfrak{R}^{(\Gamma i L q)}(\vec{r};E_\mu) = \oint_{E_\mu(\vec{k})=E} d\xi\, d\eta\, \varphi_\mu(\vec{r};E,\xi,\eta) \times \langle\xi\eta|\Gamma i L q\rangle_{E_\mu}. \tag{2.3}$$

By definition, the set $\{\langle\xi\eta|\Gamma i L q\rangle_{E_\mu}\}$ is complete and orthonormal *over the constant-energy surface*, Eq. (2.1). We set

$$\langle\xi\eta|\Gamma i L q\rangle_{E_\mu} = \frac{1}{\sqrt{\Omega}}\, e^{[i\Theta_\mu(\vec{k})]} \left|\frac{\partial(k_x,k_y,k_z)}{\partial(E,\xi,\eta)}\right|^{1/2} \times P_{Lq}^{(\Gamma i)}(\vec{k};E_\mu), \tag{2.4}$$

where $\{P_{Lq}^{(\Gamma i)}(\vec{k};E_\mu)\}$ is a complete and orthonormal set of polynomials in the fundamental domain Ω belonging to the *non-negative density function*[11] $\delta(E-E_\mu(\vec{k}))/\Omega$, i.e., such that

$$\frac{1}{\Omega}\int_\Omega d\vec{k}\,\delta(E-E_\mu(\vec{k}))\,P_{Lq}^{(\Gamma i)}(\vec{k};E_\mu)\,P_{L'q'}^{(\Gamma' i')}(\vec{k};E_\mu) = \delta_{\Gamma\Gamma'}\delta_{ii'}\delta_{LL'}\delta_{qq'}. \tag{2.5}$$

The phase factor $e^{i\Theta_\mu(\vec{k})}$ is related to the choice of the relative phase of the Bloch waves for different $\vec{k}$, to be discussed in the companion paper.

Note the close analogy between Eq. (2.3) and the familiar integral representation of the spherical Bessel (regular) function of order l[12]:

$$i^l j_l(kr) Y_{lm}(\hat{r}) = \frac{1}{4\pi}\int_{4\pi} d\hat{k}\, e^{i\vec{r}\cdot\vec{k}} Y_{lm}(\hat{k}). \tag{2.6}$$

This function constitutes the component of angular momentum l of a plane wave. It describes the motion of a particle about a "center" in empty space. The corresponding constant-energy surface $E=k^2$ has spherical shape. Equation (2.6) still forms part of the solution when a spherical potential of bounded range is turned on. In this case, the state of a particle with angular momentum l is described, beyond the range of the potential, by a superposition of the spherical Bessel function (2.6) and of the spherical Neumann (irregular) function. The latter can also be expressed by means of an integral of the form (2.6), but the vector $\vec{k}$ now ranges over an appropriate surface in the complex domain.[13]

The wave packet (2.3) generalizes Eq. (2.6) to nonspherical constant-energy surfaces. The corresponding generalization of the spherical Neumann function will be carried out in a future paper. The

set $\{\langle \xi\eta | \Gamma i L q\rangle_{E_\mu}\}$ can thus be described as the *harmonics of the constant-energy surface.*[14]

The rest of the paper will deal with a numerical example of the construction of the orthonormal polynomials $P_{Lq}^{(\Gamma i)}(\vec{k}; E_\mu)$.

III. NUMERICAL CALCULATION OF THE POLYNOMIALS $P_{Lq}^{(\Gamma i)}(\vec{k}; E_\mu)$

A. Orthogonalization procedure

To construct the set of orthonormal polynomials in Ω belonging to the non-negative weight function $\delta(E - E_\mu(\vec{k}))/\Omega$ we may start from *any* convenient set of *linearly independent* polynomials in $\vec{k}$. Following Ref. 3, we choose a set of polynomials $\{v_{ls\lambda}^{(\Gamma i)}(\vec{k})\}$ that are (i) real[15]; (ii) homogeneous of degree l in the components of $\vec{k}$; (iii) symmetry adapted, i.e., transforming under the point-group operations according to the ith row of the irreducible representation Γ; and (iv) normalized so that

$$e^{i\vec{r}\cdot\vec{k}} = \sum_{\Gamma i}\sum_{ls\lambda} i^l v_{ls\lambda}^{(\Gamma i)}(\vec{r}) v_{ls\lambda}^{(\Gamma i)}(\vec{k}) . \tag{3.1}$$

Each polynomial $v_{ls\lambda}^{(\Gamma i)}(\vec{k})$ can be factored as the product of k^l and of a symmetry-adapted spherical harmonic of degree $l-2s$, which represents its angular dependence; s need not vanish because the constant-energy surface is not spherical. The index λ distinguishes different harmonics of the same degree and symmetry species.

Symmetry-adapted spherical harmonics have been first introduced for the cubic group by Von der Lage and Bethe[16] who called them Kubic harmonics. Their generalization to all crystallographic point groups, mainly by Altmann and collaborators, has led to a complete tabulation in Chap. 2 of Ref. 29.

We indicate the overlap integral of any pair of real functions $f^{(\Gamma i)}(\vec{k})$ and $g^{(\Gamma i)}(\vec{k})$, over the constant-energy surface $E_\mu(\vec{k}) = E$ as

$$\langle f | W_{E_\mu}(\Gamma) | g\rangle \equiv \frac{1}{\Omega}\int_\Omega d\vec{k}\,\delta(E - E_\mu(\vec{k})) \times f^{(\Gamma i)}(\vec{k}) g^{(\Gamma i)}(\vec{k}) . \tag{3.2}$$

Each polynomial $P_{Lq}^{(\Gamma i)}(\vec{k}; E_\mu)$ is then constructed as a linear combination of the $v_{ls\lambda}^{(\Gamma i)}(\vec{k})$ with $l \le L$ by the following *recursion procedure.* We start with the lowest degree l_0 that occurs for the given Γ in the process of symmetry adapting the spherical harmonics. Generally l_0 is nondegenerate and we can set

$$P_{l_0}^{(\Gamma i)}(\vec{k}; E_\mu) = v_{l_0 0}^{(\Gamma i)}(\vec{k}) / \langle v_{l_0 0} | W_{E_\mu}(\Gamma) | v_{l_0 0}\rangle^{1/2} . \tag{3.3}$$

For each $L > l_0$, we first orthogonalize all the $v_{ls\lambda}^{(\Gamma i)}(\vec{k})$ with $l = L$ to all the $P_{L'q'}^{(\Gamma i)}(\vec{k}; E_\mu)$ with $L' < L$ and define

$$u_{Ls\lambda}^{(\Gamma i)}(\vec{k}) \equiv v_{Ls\lambda}^{(\Gamma i)}(\vec{k}) - \sum_{L'q'}^{L'<L} P_{L'q'}^{(\Gamma i)}(\vec{k}; E_\mu) \times \langle P_{L'q'} | W_{E_\mu}(\Gamma) | v_{Ls\lambda}\rangle . \tag{3.4}$$

We then expand

$$P_{Lq}^{(\Gamma i)}(\vec{k}; E_\mu) = \sum_{s\lambda} u_{Ls\lambda}^{(\Gamma i)}(\vec{k}) d_{s\lambda}^{(Lq)} , \tag{3.5}$$

where the coefficients $\vec{d}^{(Lq)}$ are to be determined as the eigenvectors of the positive semidefinite, real, and symmetric matrix:

$$\langle u_{Ls\lambda} | W_{E_\mu}(\Gamma) | u_{Ls'\lambda'}\rangle . \tag{3.6}$$

The $\vec{d}^{(Lq)}$ are normalized in accordance with

$$\overline{W}_{Lq}(\Gamma) \sum_{s\lambda} d_{s\lambda}^{(Lq)2} = 1 , \tag{3.7}$$

where $\overline{W}_{Lq}(\Gamma)$ is the corresponding eigenvalue of the matrix (3.6). The residual sign arbitrariness of each $\vec{d}^{(Lq)}$ is removed by requiring its component $d_{s_{\max}}^{(Lq)}$ to be positive.

Both the overlap integrals in Eq. (3.4) and the matrix elements (3.6) can be expressed in terms of the elementary structural parameters

$$\langle v_{ls\lambda} | W_{E_\mu}(\Gamma) | v_{l's'\lambda'}\rangle . \tag{3.8}$$

These are the quantities which we will calculate by numerical integration. Specifically, we restrict our attention to the examples listed in Table I for the irreducible representations A_{1g}, T_{1u}, and E_g of the cubic group up to $L_{\max} = 4$. This sample of polynomials appears sufficient to illustrate general properties that are of interest at this time. Larger samples may, of course, become necessary, for example, if one were to represent a nonsmooth function of $\vec{k}$ over the constant-energy surface.

TABLE I. Examples of basis polynomials for the group O_h (from Appendix of Ref. 3).

l	A_{1g}	T_{1u} ($i = 1, 2, 3$)	E_g ($j = 1, 2$)
0	v_{00}		
1		$v_{10}^{(i)}$	
2	v_{21}		$v_{20}^{(j)}$
		$v_{30}^{(i)}$	
3		$v_{31}^{(i)}$	
	v_{40}		$v_{40}^{(j)}$
4	v_{42}		$v_{41}^{(j)}$

B. Parametrization of the *s-d* bands of copper

We performed the calculation for the *s-d* bands of metallic copper, for theoretical and experimental reasons. On the theoretical side, the band properties of Cu have been extensively investigated and it is believed that Cu is probably the best test for the band theory of metals.[17] On the experimental side, the photoabsorption spectrum of Cu is so well known that it is taken as a reference spectrum for calibrations.

The band information relevant to our problem, namely, the family of constant-energy surfaces (2.1), was obtained by fitting the *ab initio* APW band calculation of Burdick[18] using the Slater-Koster interpolation scheme.[19] This method has proved applicable to many types of crystals having wide bands, which would not normally be considered to be tightly bound,[20,21] and has been used recently[22] to calculate two-dimensional band structures related to surfaces.

This procedure provides a cheap and accurate band structure $E_\mu(\vec{k})$ over the whole Brillouin zone but fails to provide the Bloch waves $\varphi_\mu(\vec{r};\vec{k})$ because it determines only the integrals

$$\langle a_i(\vec{r})|\hat{H}_c|a_j(\vec{r}-\vec{n})\rangle\,, \tag{3.9}$$

$\vec{n}$ being a lattice vector of the crystal, rather than the atomiclike orbitals $\{a_i(\vec{r})\}$ themselves. One might envisage calculating these orbitals by Kohn's variational method[23] which evaluates a set of atomiclike orbitals $\{a_i(\vec{r})\}$ *ab initio* from which all relevant informations about the band structure can be obtained. In a similar approach Chadi[24] has shown that the bands of Ge, Si, and GeAs can be calculated with good accuracy from a few optimized Slater orbitals.

The fitting of the lowest six bands at 38 points in the basic domain ω (or irreducible wedge) of the Brillouin zone has been carried out by simultaneous variation of the parameters following the techniques discussed by Connolly.[20] All the interaction integrals (3.9) up to the second-nearest neighbors have been included for a total of 32 different parameters. The total rms deviation of the fit is 8 mRy, which is within the accuracy of the *ab initio* calculation.[18] The "best estimate values" of the parametric integrals are listed in Table II.[25] We used these values to evaluate the rms deviation for all the 84 points in the Brillouin zone where the first six *ab initio* bands are known. The value of 8 mRy was again obtained; only 10 points were found to have partial rms deviation larger than 10 mRy.

C. Integration procedure

We calculated the integrals

$$\langle v_{l_1 s_1 \lambda_1}|W_{E_\mu}(\Gamma)|v_{l_2 s_2 \lambda_2}\rangle = \frac{1}{\Omega}\int_\Omega d\vec{k}\,\delta(E-E_\mu(\vec{k}))v^{(\Gamma i)}_{l_1 s_1 \lambda_1}(\vec{k})v^{(\Gamma i)}_{l_2 s_2 \lambda_2}(\vec{k}) \tag{3.10}$$

by the quadratic interpolation scheme[8] (QUAD) for the examples listed in Table I using the dispersion relations $E_\mu(\vec{k})$ thus determined.

TABLE II. "Best estimate" values of the parametric integrals (in Ry).

$E_{s,s}(000)$	−0.187 924	$E_{z,x^2-y^2}(011)$	−0.003 237
$E_{s,s}(110)$	−0.072 737	$E_{x,x}(000)$	0.531
$E_{s,xy}(110)$	−0.014 983	$E_{x,x}(110)$	0.104
$E_{s,3z^2-r^2}(110)$	−0.006 167	$E_{x,x}(011)$	−0.001
$E_{xy,xy}(000)$	−0.579 919	$E_{x,y}(110)$	0.101 505
$E_{xy,xy}(110)$	−0.019 662	$E_{s,s}(200)$	0.010 271
$E_{xy,xy}(011)$	0.006 759	$E_{s,3z^2-r^2}(002)$	−0.008 364
$E_{xy,xz}(011)$	0.012 393	$E_{xy,xy}(200)$	0.003 904
$E_{xy,3z^2-r^2}(110)$	0.011 119	$E_{xy,xy}(002)$	−0.000 040
$E_{3z^2-r^2,3z^2-r^2}(000)$	−0.575 699	$E_{3z^2-r^2,3z^2-r^2}(002)$	−0.007 245
$E_{3z^2-r^2,3z^2-r^2}(110)$	−0.009 420	$E_{x^2-y^2,x^2-y^2}(002)$	0.000 598
$E_{x^2-y^2,x^2-y^2}(110)$	0.018 213	$E_{s,x}(200)$	−0.003 851
$E_{s,x}(110)$	−0.073 195	$E_{x,xy}(020)$	−0.000 392
$E_{x,xy}(110)$	0.001 886	$E_{z,3z^2-r^2}(002)$	0.009 268
$E_{x,xy}(011)$	−0.023 928	$E_{x,x}(200)$	0.029 783
$E_{z,3z^2-r^2}(011)$	−0.025 669	$E_{y,y}(200)$	0.013 203

It has been already stressed[8] that, mainly for complicated band structures like those of transition metals, a "quadratic" interpolation scheme might be superior to any method which expands the eigenvalues $E_\mu(\vec{k})$ locally only to first order.[26] In fact, a large number of critical points occur in the band structure of transition metals. Analytic critical points are treated exactly by the QUAD scheme while in a neighborhood of a nonanalytical critical point a *smoothing* of the singularity is performed (for instance, a crossing of two bands which might occur along special directions in the Brillouin zone is approximated by two parabolas). This operational trend matches the considerations we made in Sec. I.

From a practical point of view, the QUAD scheme can be easily adapted to the calculation of integrals other than the density of states but involving arbitrary functions of the $\vec{k}$ vector, such as those in (3.10). On the other hand, the simple summation over a few "special points"[27] in the Brillouin zone cannot be used because the functions in the integrand of (3.10) are neither smooth nor periodic, with the periodicity of the reciprocal lattice.

As it is always convenient to take full advantage of the symmetry of the Brillouin zone (the Wigner-Seitz unit cell of reciprocal lattice), the integral (3.10) should rather be written as

$$\langle v_{l_1 s_1 \lambda_1} | W_{E_\mu}(\Gamma) | v_{l_2 s_2 \lambda_2} \rangle = \frac{1}{\omega} \int_\omega d\vec{k}\, \delta(E - E_\mu(\vec{k})) \left(\frac{1}{n(\Gamma)} \sum_{j=1}^{n(\Gamma)} v_{l_1 s_1 \lambda_1}^{(\Gamma j)}(\vec{k}) v_{l_2 s_2 \lambda_2}^{(\Gamma j)}(\vec{k}) \right). \tag{3.11}$$

Here ω stands for *any* basic domain in the Brillouin zone (or any number of them) and $n(\Gamma)$ is the dimension of the irreducible representation Γ. The function in braces is in fact an invariant under all operations of the point group of the crystal.[28] Specifically, this function is an invariant polynomial, homogeneous of (even) degree $l_1 + l_2$ in $\vec{k}$. It can therefore be expressed as a linear combination of the totally symmetric symmetry-adapted spherical harmonics, $X_{A_{1g}\lambda}^{(l)}(\hat{k})$, of degree $l \leq l_1 + l_2$, multiplied by $k^{l_1+l_2}$. For example[29]:

$$\frac{1}{3} \sum_{j=1}^{3} v_{30}^{(T_1 u^j)}(\vec{k}) v_{30}^{(T_1 u^j)}(\vec{k}) = k^6 \frac{\sqrt{4\pi}}{11!!} \left[\left(\frac{2}{13} \right)^{1/2} 75 X_{A_{1g}}^{(6)}(\hat{k}) + \frac{189}{\sqrt{21}} X_{A_{1g}}^{(4)}(\hat{k}) + 99 X_{A_{1g}}^{(0)}(\hat{k}) \right]. \tag{3.12}$$

It follows that one has to evaluate by the Monte Carlo method only a *minimal set* of independent integrals. For instance, in order to generate the 35 orthonormal polynomials $P_{Lq}^{(\Gamma i)}(\vec{k}; E_\mu)$ wtih $L \leq 4$, one would need to know 31 integrals of the type (3.10). However, these integrals can be expressed in terms of only 11 independent integrals belonging to the minimal set.

IV. DISCUSSION OF THE NUMERICAL RESULTS

Initial tests of the program were conducted assuming a quadratic, spherically symmetric dispersion relation $E(\vec{k}) = k^2$. A mesh size of $\frac{1}{8}$ of the Γ to X distance was found necessary and sufficient to contain within our statistical fluctuations a known systematic error of the QUAD scheme,[30] namely, a spurious valley in the density of states followed by a spurious peak near the edge of the Brillouin zone. It was also verified that the spherical symmetry reduces the number of independent polynomials of degree l from $\frac{1}{2}(l+1)(l+2)$ to $2l+1$, by causing certain polynomials to vanish identically *on* the constant-energy surface. This occurs, e.g., for the second order of polynomials $u_{21}^{(A_{1g})}(\vec{k}) = (k^2 - \langle k^2 \rangle_E / \langle 1 \rangle_E)/\sqrt{6}$. These checks were successful only when all averages were taken over the same statistical sample.

The parameters of the calculation for the s-d bands of Cu were chosen as follows:

(i) The linear size of the cubical cells was fixed to $\frac{1}{8}$ of the distance from Γ to X. This corresponds to loading the eigenvalues $E_\mu(\vec{k})$ at 505 points in the basic domain.

(ii) The spectral region from 0.2 to 0.8 Ry, above the absolute minimum of the lowest band, was explored. We then partitioned this energy interval into 100 histogram boxes of width 6 mRy.

(iii) The number of Monte Carlo sampling points was fixed at $8^3 \times 200 = 102\,400$. The average statistical error then ranges from 1.3% for the narrowest band to 3.3% for the conduction band.

The calculations of the integrals (3.10) for the basis polynomials listed in Table I took about 8 min on an IBM 370/195 computer. Figure 1 reports the density of states contributed by the six lowest bands (not counting the spin degeneracy). The position of the Fermi level was determined to be $E_F = 0.653 \pm 0.003$ Ry, which coincides, within the rms error of our fitting (8 mRy), with the value of 0.659 Ry obtained by Burdick's *ab initio* APW calculation, whose results served as input for the present work.

The overlap integrals, which appear in Eq. (3.4), and the expansion coefficients of Eq. (3.5), were calculated up to $l = 4$ for the three irreducible representations listed in Table I. These $\sim 10^4$ numbers can be supplied on request. The following characteristic features of the orthonormal set of

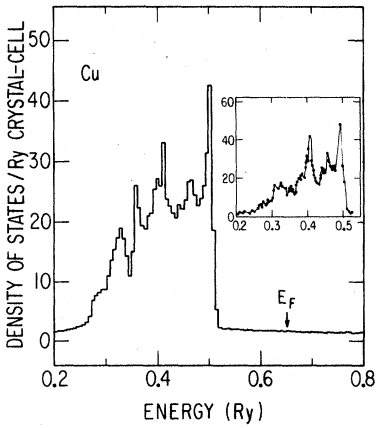

FIG. 1. Density of states contributed by the s-d bands of Cu. The statistical sample contains 102 400 Monte Carlo points; the width of the histogram boxes is 6 mRy. The Fermi level is at 0.653 ± 0.003 Ry. The inset shows, for comparison, Fig. 7 of F. M. Mueller, Phys. Rev. 153, 659 (1967).

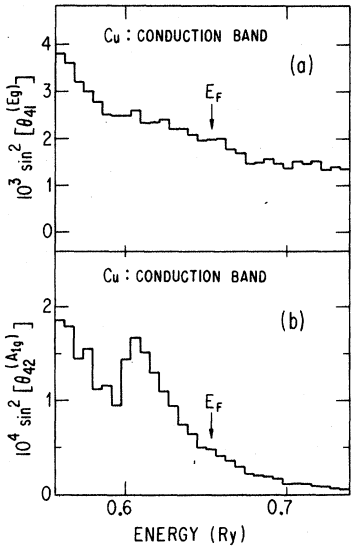

FIG. 2. Square of the sine of the "angle" between the basis polynomials (a) $v_{41}^{(E_g j)}(\vec{k})$, (b) $v_{42}^{(A_1 g)}(\vec{k})$ and the subspace with $L' < 4$ is shown vs the energy about the Fermi level. At E_F, $\theta_{42}^{(A_{1g})} \sim 0.5°$ and $\theta_{41}^{(E_g)} \sim 2.5°$.

polynomials are noted.

(a) As mentioned above, all the

$$\sum_{s=0}^{[l/2]} [2(l-2s)+1] = \tfrac{1}{2}(l+1)(l+2) \tag{4.1}$$

polynomials $u_{Ls\lambda}^{(\Gamma i)}(\vec{k})$ of maximum degree $L = l$ are linearly independent over an arbitrary constant-energy surface, but they reduce to $2l+1$ in the limit of spherical symmetry (here $[l/2]$ means integer part of $l/2$). This is because all $u_{Ls\lambda}^{(\Gamma i)}(\vec{k})$ with $s > 0$ vanish identically in the spherical limit. The ratios

$$\sin^2[\theta_{Ls\lambda}^{(\Gamma)}(E_\mu)] \equiv \frac{\langle u_{Ls\lambda} | W_{E_\mu}(\Gamma) | u_{Ls\lambda} \rangle}{\langle v_{Ls\lambda} | W_{E_\mu}(\Gamma) | v_{Ls\lambda} \rangle}, \tag{4.2}$$

with $s > 0$ can then be taken as measures of the degree of linear independence of the set $\{u_{Ls\lambda}^{(\Gamma i)}(\vec{k})\}$, for given Γ and L. As a geometrical analog, the parameter $\theta_{Ls\lambda}^{(\Gamma)}$ can be interpreted as the "angle" between the vector $v_{Ls\lambda}^{(\Gamma i)}(\vec{k})$ and the subspace with $L' < L$. The vector $u_{Ls\lambda}^{(\Gamma i)}(\vec{k})$ is the component orthogonal to the subspace $L' < L$. It thus vanishes for $\theta_{Ls\lambda}^{(\Gamma)} = 0$. We therefore, expect a quasispherical surface to be characterized typically by small values of this parameter. In Fig. 2 we report examples of the ratios (4.2) for $L = 4$ and $\Gamma \equiv \{A_{1g}, E_g\}$, for the conduction band of Cu in an energy window of 0.180 Ry about the Fermi level. We see that the lack of angular dependence makes the polynomial $v_{42}^{(A_1 g)}(\vec{k})$ more nearly linearly dependent on the subspace with $L' < 4$ than the polynomial $v_{41}^{(E_g j)}(\vec{k})$, for $\vec{k}$ restricted to a constant-energy surface about the Fermi level. At E_F, $\theta_{42}^{(A_1 g)} \sim 0.5°$. For a narrow d band with complicated many-sheet surfaces, $\theta_{42}^{(A_1 g)}$ can become as large as $\sim 10°$.

(b) By the same token, the parameter (4.2) will increase as the constant-energy surface becomes increasingly warped when approaching the Brillouin-zone boundary. In the example of a nearly-free electron, the ratio (4.2) would vanish as long as k^2 is constant over an energy surface even if this surface is interrupted by the intersection with the zone boundary, but warping would in fact prevent (4.2) from vanishing.

(c) A related set of parameters of the constant-energy surface which is worth discussing consists of the eigenvalues $\overline{W}_{Lq}(\Gamma)$ of the overlap matrix (3.6). As shown in Ref. 3, the density of states at the $\vec{n}$ crystal cell can be subdivided into contributions from the various multipoles about the "central" cell. The density of states contributed by the $\Gamma i L q$ multipole can be expanded then into a power series in $\vec{n}$. If one retains only the terms of the lowest degree $2L$ in such an expansion, the density of states contributed by the $\Gamma i L q$ multipole turns out to be proportional to the corresponding eigenvalue $\overline{W}_{Lq}(\Gamma)$ of the matrix (3.6). *This eigenvalue thus represents, to lowest order, the weight of partitioning the density of states into multipoles.* Figures 3 and 4 show $\overline{W}_{Lq}(\Gamma)$ again for $L = 4$ and $\Gamma \equiv \{A_{1g}, E_g\}$, $(q = +, -)$ about the Fermi level. One can see that $\overline{W}_{4+}(A_{1g})/\overline{W}_{4-}(A_{1g}) \sim 10^3$, while this ratio reduces to ~ 10 for a d band.

ACKNOWLEDGMENTS

I wish to express my deep gratitude to Professor U. Fano, who suggested this problem, for his

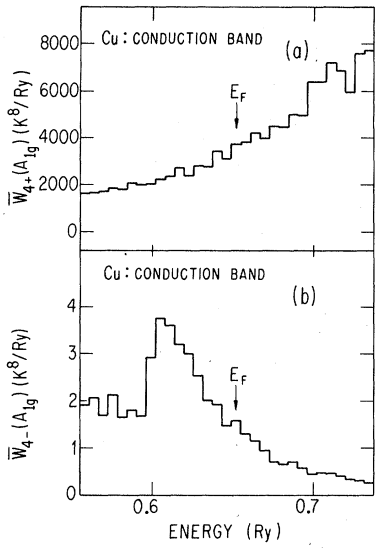

FIG. 3. The highest (+) and the lowest (−) eigenvalues, (a) and (b), respectively, of the overlap matrix (3.6) are shown for $L=4$ and $\Gamma=A_{1g}$ about the Fermi level. [Note: the $\vec{k}$ vector in the integrals (3.6) has been expressed in $\pi/4a$ units, a being the lattice constant for copper.]

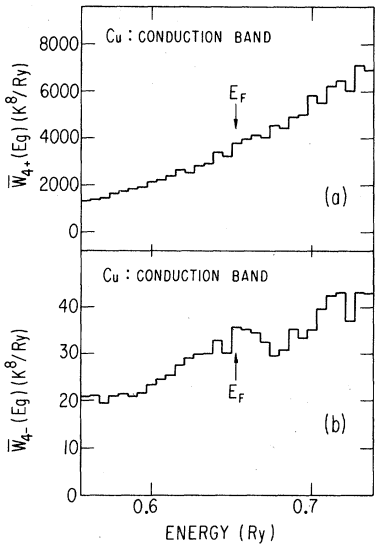

FIG. 4. Same as in Fig. 3, for $\Gamma=E_g$.

continuous guidance and support, and for his help in preparing this manuscript. I also with to thank Professor M. H. Cohen for many stimulating discussions, Dr. S. G. Das for providing the numerical programs and for help during the initial stage of the calculations, and Dr. D. D. Koelling for discussions on the QUAD scheme. This work was supported by the U. S. ERDA, Division of Physical Research, under Contract No. C00-1674-131. This paper was presented as a thesis to the Department of Physics, The University of Chicago, in partial fulfillment of the requirements for the Ph.D. degree.

[1]U. Fano, Phys. Rev. Lett. 31, 234 (1973).
[2]U. Fano, in *Vacuum Ultraviolet Radiation Physics*, edited by E. E. Koch, R. Haensel, and C. Kunz (Vieweg, Braunschweig, 1974), p. 84.
[3]G. Strinati and U. Fano, J. Math. Phys. 17, 434 (1976).
[4]M. Brown, R. E. Peierls, and E. A. Stern, Phys. Rev. B 15, 738 (1977).
[5]D. J. Phelps, R. A. Tilton, and C. P. Flynn, Phys. Rev. B 14, 5254 (1976).
[6]For a description of atomic quantum-defect theory, see C. M. Lee, Phys. Rev. A 10, 584 (1974), and references therein.
[7]G. F. Koster, Phys. Rev. 95, 1436 (1954); J. Callaway, J. Math. Phys. 5, 783 (1964); Phys. Rev. 154, 515 (1967); F. Gautier and P. Lenglart, Phys. Rev. 139, A705 (1965).
[8]F. M. Mueller, J. W. Garland, M. H. Cohen, and K. H. Bennemann, Ann. Phys. 67, 19 (1971).
[9]The reasons for this choice will be discussed in Sec. III of the companion paper.
[10]An extensive summary of geometrical properties of constant-energy surfaces can be found in I. M. Lifshits, M. Ya. Azbel', and M. I. Kaganov, *Electron Theory of Metals* (Consultants Bureau, New York, 1973).
[11]R. Courant and D. Hilbert, *Methods of Mathematical Physics* (Interscience, New York, 1966), p. 87.
[12]See, for instance, A. R. Edmonds, *Angular Momentum in Quantum Mechanics* (Princeton U. P., Princeton, N.J., 1960), p. 81.
[13]P. M. Morse and H. Feshbach, *Methods of Theoretical Physics* (McGraw-Hill, New York, 1953), Vol. I, p. 625.
[14]The usefulness of these harmonics for the treatment of quite different classes of physical phenomena has been pointed out by P. B. Allen, Phys. Rev. B 13, 1416 (1976).
[15]This is possible for those crystal point groups for which the matrices of the representations can be taken to be real.
[16]F. C. Von der Lage and H. A. Bethe, Phys. Rev. 71, 612 (1947).
[17]B. Segall, Phys. Rev. 125, 109 (1962).
[18]G. A. Burdick, Phys. Rev. 129, 138 (1963).
[19]J. C. Slater and G. F. Koster, Phys. Rev. 94, 1498 (1954).
[20]J. W. D. Connolly, in *Electronic Density of States*, Natl. Bur. Stand. Special Publ. No. 323 (U.S. GPO, Washington D.C., 1971), p. 27.
[21]S. G. Das, Phys. Rev. B 13, 3978 (1976); B. Chakraborty, W. E. Pickett, and P. B. Allen, Phys. Rev. B 14, 3227 (1976).
[22]K. S. Sohn, D. G. Dempsey, L. Kleinman, and Ed Ca-

ruthers, Phys. Rev. B 13, 1515 (1976); N. V. Smith and L. F. Mattheiss, Phys. Rev. Lett. 37, 1494 (1976).
[23]W. Kohn, Phys. Rev. B 7, 4388 (1973).
[24]D. J. Chadi, Phys. Rev. B 16, 3572 (1977).
[25]All matrix elements of the Slater-Koster Hamiltonian were made real by taking the orbitals $a_i(\vec{r})$ with even parity ($4s, 3d$) as real and those with odd parity ($4p$) as purely imaginary. This fact has to be taken into account when using Table II of Ref. 19.
[26]We plan to use in the future also the "tetrahedron method" [J. Rath and A. J. Freeman, Phys. Rev. B 11, 2109 (1975)]. A new version of the method, which will include a quadratic interpolation, is in progress [S. G. Das (private communication)].
[27]D. J. Chadi and M. L. Cohen, Phys. Rev. B 8, 5747 (1973).
[28]This is referred to as the "generalized Unsöld theorem." See, for instance, M. Tinkham, *Group Theory and Quantum Mechanics* (McGraw-Hill, New York, 1964), p. 80.
[29]We follow the notation of C. J. Bradley and A. P. Cracknell, *The Mathematical Theory of Symmetry in Solids* (Clarendon, Oxford, England, 1972).
[30]E. B. Kennard, D. Koskimaki, J. T. Waber, and F. M. Mueller, in *Electronic Density of States*, Natl. Bur. Stand. Special Publ. No. 323 (U.S. GPO, Washington, D.C., 1971), p. 795.